

## P5A.8

### FINE-SCALE RADAR OBSERVATIONS OF A DRYLINE DURING THE INTERNATIONAL H<sub>2</sub>O PROJECT

Christopher C. Weiss<sup>\*</sup> and Howard B. Bluestein  
University of Oklahoma  
Norman, Oklahoma

Andrew L. Pazmany  
ProSensing  
Amherst, Massachusetts

#### 1. INTRODUCTION

The Southern Plains dryline has long been identified as a location favorable for the development of deep moist convection. Thunderstorms initiated at the dryline often are in an environment conducive for supercells, with the attendant threat of large hail, damaging winds and tornadoes. Although progress has been made in our understanding of the dryline, the kinematic structure of the boundary is still unclear. Any consistent success in the prediction of convective initiation on the dryline relies on the precise specification of the wind field on very small spatial scales, particularly in the dryline convergence zone (DCZ) where parcels must ascend to the level of free convection (LFC) for initiation to occur.

During the spring of 2002, the International H<sub>2</sub>O Project (IHOP) sought to resolve the kinematics of the dryline interface, particularly in the context of convective initiation. Ground-based (e.g., S-Pol, SMART-Radar (SR1), DOWs) and airborne-based (e.g., ELDORA) radar platforms were used to collect data. On May 22, 2002, in conjunction with these platforms, the 3-mm wavelength mobile Doppler radar from the University of Massachusetts at Amherst (UMass) obtained very-high resolution RHI data across a dryline in the eastern Oklahoma

panhandle. The very narrow beamwidth (0.18 deg) of the antenna permitted ultra-fine scale measurements of the dryline boundary, with height and range resolutions of 5 m and 30 m, respectively, at a distance 1 km from the radar.

#### 2. DATA COLLECTION METHOD

The following deployment strategies were utilized in the data collection:

1) Velocity Azimuth Display (VAD) – stationary collection of data taken at ~45 deg elevation angle. The antenna was rotated horizontally through ~ 220 deg portion of a cone (limited by the hardware of the positioner).

2) Vertical antenna – antenna pointed at ~ 90 deg and driven across the boundary.

3) Stationary RHI – stationary data collection in which antenna rotated from ~0-90 deg (Fig. 1)

4) Rolling RHI – 0-90 deg RHIs collected with the truck in motion (Fig. 1). Radar velocity must be adjusted for truck motion.

A boresighted camera was mounted on the W-band dish to collect simultaneously video during most of the deployments. This video was instrumental in identifying regions of cloud cover. Further, it allowed the detection of ground targets. The video time stamp was synchronized with the data acquisition system.

Leg	Time (UTC)	Scan strategy	Other operational radar platforms (portion of leg available in UTC)
1	2012-2050	Rolling RHI (westward truck motion)	DOW2 (-2035), DOW3 (-2017), SR1 (-2024)
2	2109-2151	Rolling RHI (eastward truck motion)	DOW2 (2127-), DOW3 (2129-), SR1 (2136-)
3	2222-2233	Vertical antenna (westward truck motion)	DOW2, DOW3
4	2242-2325	Stationary RHI	DOW2, DOW3, SR1 (2254-)
5	2345-0001	Rolling RHI (eastward)	DOW2, DOW3, SR1
6	0007-0036	Rolling RHI (westward)	DOW2, DOW3, SR1
7	0036-0045	Stationary RHI	DOW2, DOW3, SR1

Table 1 – Data collection periods and scan strategy for the UMass W-band radar on 22 May 2002

<sup>\*</sup>Corresponding author address: Christopher C. Weiss, School of Meteorology, Univ. of Oklahoma, Norman, OK 73019; e-mail: cweiss@ou.edu

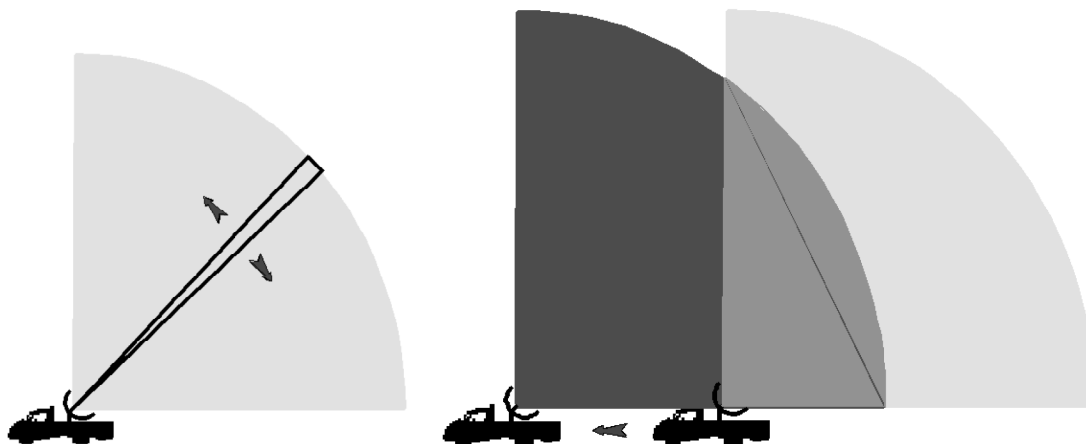


Fig. 1 – Schematic of Stationary RHI (left) and Rolling RHI (right) scanning strategy

### 3. PRELIMINARY ANALYSES

#### a. Leg 3 (2222-2233 UTC)

A vertical antenna deployment was performed as the UMass truck drove westward across, and approximately normal to, the dryline boundary.

The reflectivity composite of leg 3 (Fig. 2) shows clearly a maximum in the lowest 2 km AGL, coincident with the location of the DCZ. The tilt of this interface was approximately 45 deg above the horizon over the lowest 2 km AGL. An area of high reflectivity (region 1) was noted within the DCZ, approximately 800 m in width and depth, and centered at 1 km AGL. Other areas of high reflectivity were evident to the west of the dryline (regions 2, 3 and 4). The boresighted camera confirmed the existence of cumulus convection in these regions. In fact, cumulus clouds were first evident *immediately* to the west of the surface dryline location (region 2); none were seen in the first 6 km east of the dryline.

A maximum in upward motion ( $w \sim 7-9 \text{ m s}^{-1}$ ) was evident (Fig. 2) in region 1 (DCZ). Upward vertical motion of  $3-7 \text{ m s}^{-1}$  was coincident with the cumulus convection in regions 2, 3 and 4. The periodic nature of the cumulus clouds west of the dryline plus the broad downward motion ( $w \sim -1 \text{ to } -3 \text{ m s}^{-1}$ ) west of regions 3 and 4 (Fig. 2) suggested that these areas may have been horizontal convective rolls (HCRs) (e.g., Atkins et al. 1998). Since the surface wind was from approximately 200 deg to the west of the dryline (not shown), the cross-section plane of the W-band would have been close, but not exactly perpendicular, to these HCRs.

A few areas of downward motion were of interest. A downward intrusion of air (likely dry air from the elevated mixed layer) was indicated

approximately 1 km to the east of the surface dryline, at about 1 km AGL (Fig. 5). A larger area of weak downward motion (region 6) was seen 5 km to the east of the surface dryline. Also, an area of gentle downward motion ( $w \sim -1 \text{ to } -3 \text{ m s}^{-1}$ ) was found 5-8 km to the west of the surface dryline position (region 7). These areas of subsiding air are consistent with that found in prior studies using airborne Doppler data (e.g., Atkins et al. 1998; Weiss and Bluestein 2002), but are seen in greater detail in this study. Downward vertical motion to the east of the dryline has been shown to bring dry air to the surface, and may explain the forward (eastward) advancement of some drylines as well as the apparent “stepped” nature of these boundaries (e.g., Hane et al. 1993). Downward motion to the west of the dryline has been hypothesized to affect convergence at the base of the DCZ (Weiss and Bluestein 2002).

#### b. Leg 7 (0036-0045 UTC)

The UMass W-band remained stationary at 0036 UTC as the dryline retrograded westward through the position of the radar. The dryline interface was clearly shown in the reflectivity and radial velocity data (Fig. 3). As expected, a weak ( $\sim 1-2 \text{ m s}^{-1}$ ) easterly component wind was evident to the east of the boundary, with localized areas of slightly stronger easterly winds. Inflections were noted at the top of the dryline interface (e.g., note the region where the radial velocity switched direction quickly over a short distance). Such inflections may be evidence of Kelvin-Helmholtz waves, owing to the sharp vertical gradient in horizontal velocity across the top of the moist layer.

## CURRENT/FUTURE WORK

Variational multiple-Doppler wind syntheses are underway that will utilize data taken with the UMass rolling RHIs and other IHOP platforms. An observation system simulation experiment (OSSE) is also being developed to guide in the construction of the variational procedure. The goal of this work is to resolve the full two-dimensional circulation normal to the dryline.

## ACKNOWLEDGMENTS

This research was funded by NSF grant ATM-9912097. We are grateful to Erik Rasmussen and Conrad Ziegler, who provided useful real-time information on dryline position. Also, we thank Bob Conzemius for his nowcast support. Brendan Fennell drove the W-band truck.

## REFERENCES

Atkins, N. T., R. M. Wakimoto, and C. L. Ziegler, 1998: Observations of the finescale structure of a dryline during VORTEX 95. *Mon. Wea. Rev.*, **126**, 525-550.

Hane, C. E., C. L. Ziegler, and H. B. Bluestein, 1993: Investigation of the dryline and convective storms initiated along the dryline: Field experiments during COPS-91. *Bull. Amer. Meteor. Soc.*, **74**, 2133-2145.

Weiss, C. C., and H. B. Bluestein, 2002: Airborne pseudo-dual Doppler analysis of a dryline-outflow boundary intersection. *Mon. Wea. Rev.*, **130**, 1207-1226.

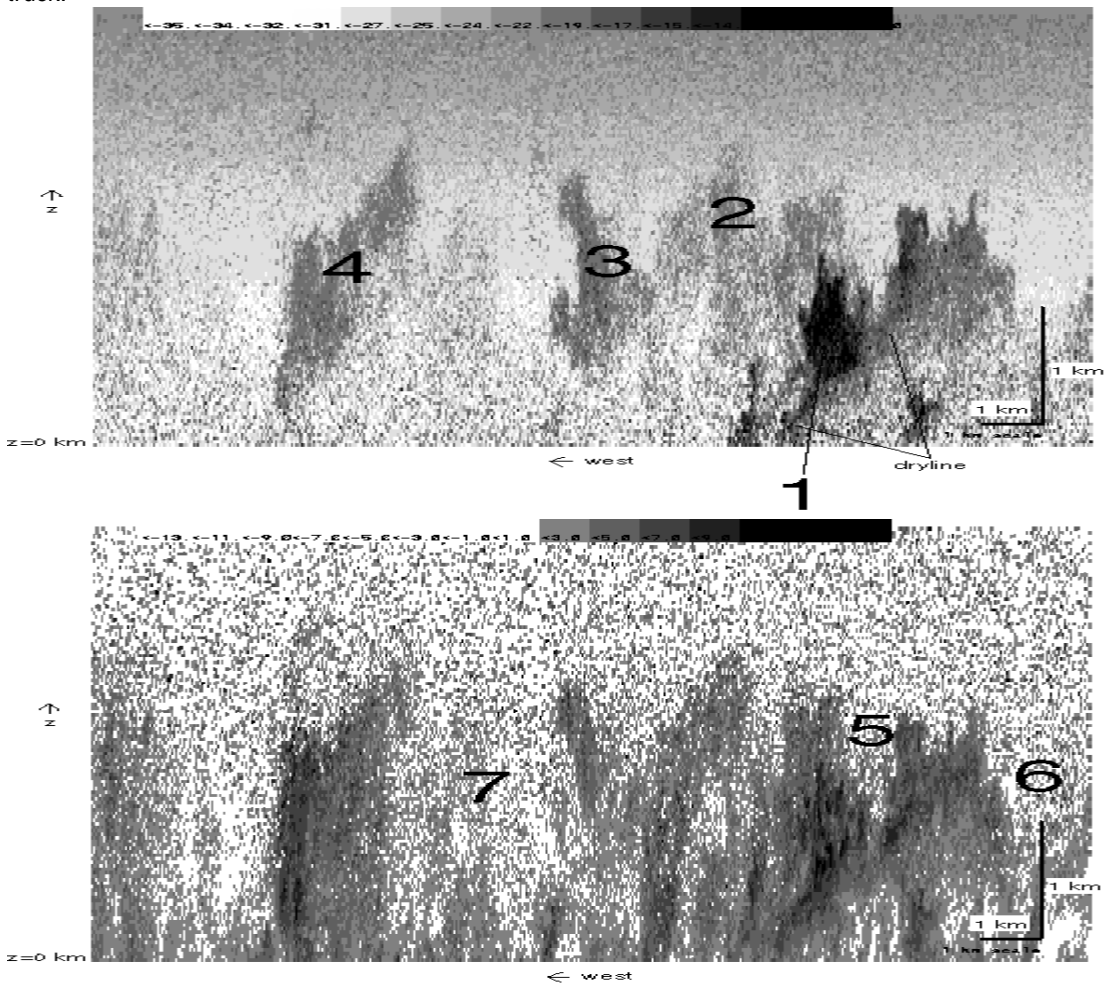


Fig. 2 – (top) UMass W-band reflectivity ( $\text{dBZ}_e$ , shaded) of the stationary dryline from a westward-moving vertical antenna deployment (leg 3, 2222-2233 UTC); (bottom) UMass W-band vertical velocity ( $\text{m s}^{-1}$ , regions greater than  $+1 \text{ m s}^{-1}$  are shaded). The domain is stretched in the vertical; note the different horizontal and vertical 1 km scales in the lower right hand corner of each display. The numeral labels are referred to in the text.

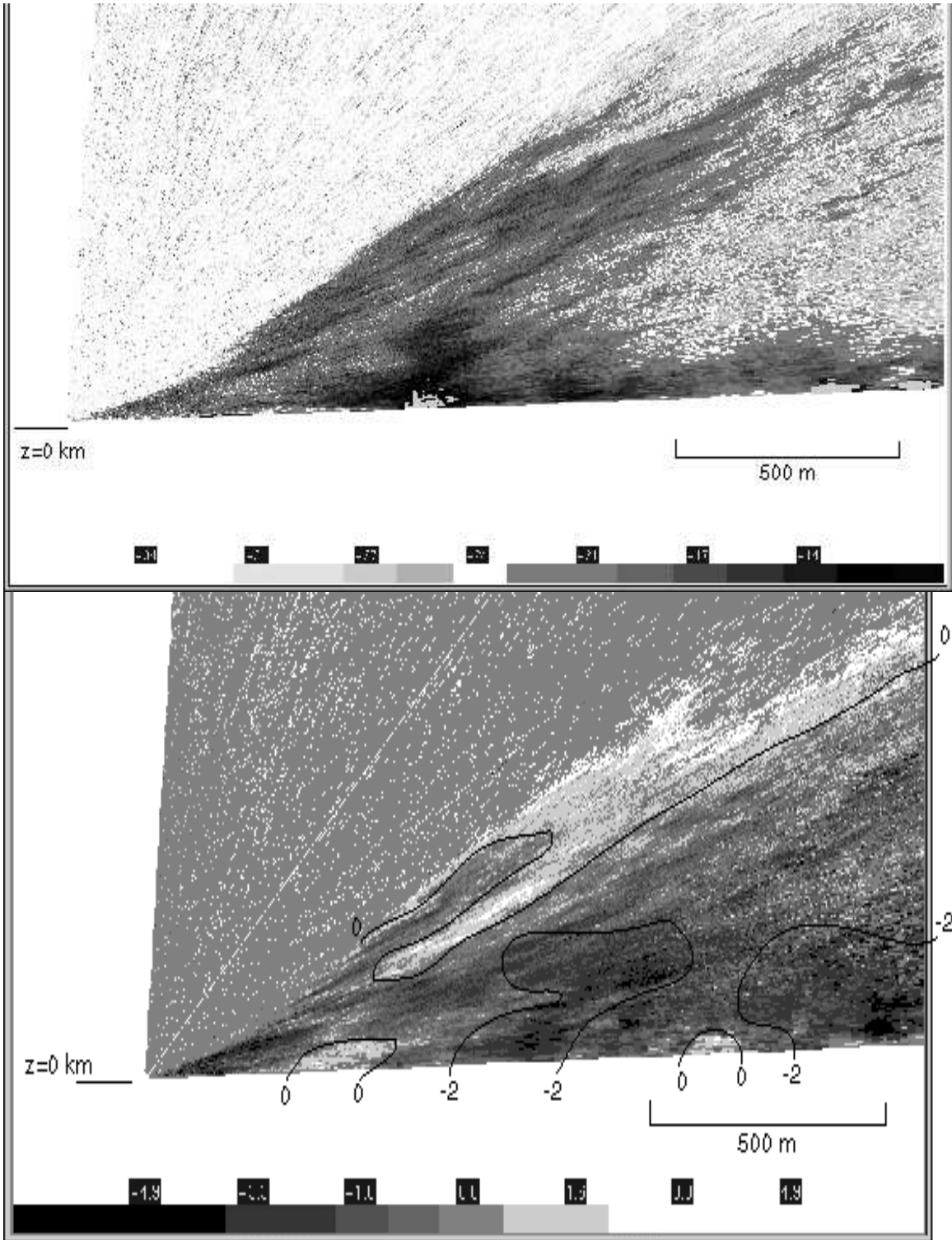


Fig. 3 – (top) UMass W-band reflectivity ( $\text{dBZ}_e$ , shaded) of the retrograding dryline at 0037 UTC from a stationary RHI deployment; (bottom) UMass W-band velocity ( $\text{m s}^{-1}$ , shaded and contoured). The radar is located in the lower left hand corner of the display. The domain is 1.6 km to the east (right) by 0.6 km in the vertical (upward).